12 March 1999

ELSEVIER

Chemical Physics Letters 302 (1999) 132–138

CHEMICAL PHYSICS LETTERS

Collisional quenching of $OH(A\,^2\Sigma^+,\ v'=0)$ by H_2O between 211 and 294 K and the development of a unified model for quenching

A.E. Bailey [a], D.E. Heard [a,*], D.A. Henderson [a], P.H. Paul [b]

[a] *School of Chemistry, University of Leeds, Leeds, LS2 9JT, UK*

[b] *Combustion Research Facility, Division 8351, Sandia National Laboratories, P.O. Box 969, Livermore, CA 94550, USA*

Received 25 November 1998; in final form 4 January 1999

Abstract

The cross-section for electronic quenching of $OH(A\,^2\Sigma^+,\ v'=0)$ by H_2O was found to increase from 82 ± 8 Å^2 at 294 K to 119 ± 11 Å^2 at 211 K. Both $OH(A\,^2\Sigma^+)$ and H_2O display relatively large dipole moments, and a 'harpooned' mechanism occurring on a Lennard-Jones potential energy surface modified to include dipole moment effects was found to reproduce the observed temperature dependence of the cross-sections in the range 211–2300 K. The model, which is general, will enable corrections for the effects of quenching on laser-induced fluorescence signals to be made with a high degree of confidence in combustion and atmospheric media.

1. Introduction

Laser-induced fluorescence (LIF) has enjoyed considerable success as a highly selective and sensitive in situ technique for the detection of the hydroxyl radical [1–3]. OH plays a central role in the chemistry of the atmosphere and in combustion media, and its detection by LIF using the strong $A\,^2\Sigma^+ - X\,^2\Pi_i$ transition has played a key role in the elucidation of complex chemical mechanisms [4,5]. Quantitative measurement of OH concentrations requires a knowledge of the rate of collisional quenching of the $A\,^2\Sigma^+$ state, which can be calculated if the cross-sections for quenching by all collision gases present are known at the temperature of the measurement. Temperatures may vary from 2500 K in flames [1] to less than 200 K in the stratosphere [6] or within free-jet expansions which sample OH in the troposphere [2,3,7]. A large body of data has been assimilated for the quenching of OH [8–10], but a notable gap in the database is the quenching cross-section by water vapour, for which data are available only at room temperature [10–14] and at selected values above 1000 K [15–17]. Water is present in significant concentrations in the atmosphere and in combustion media, and is known to be a highly efficient quencher of OH fluorescence [11]. In this Letter we report cross-section measurements for quenching by water vapour in the range 211–294 K.

Of fundamental interest is the mechanism by which the electronic energy of $OH(A\,^2\Sigma^+)$ is removed upon collision. Ab initio calculations have been carried out to determine the intermolecular interaction energy between $OH(A\,^2\Sigma^+)$ or $OH(X\,^2\Pi_i)$ and several colliders for selected config-

* Corresponding author. Fax: +44 113 233 6565; e-mail: dwayneh@chem.leeds.ac.uk

0009-2614/99/$ - see front matter
PII: S0009-2614(99)00076-7

urations and separation distances [18,19]. For some colliders conical intersections have been identified at accessible energies between the $OH(A^2\Sigma^+)$–M and $OH(X^2\Pi_i)$–M surfaces [19], which may represent the specific OH–M configuration at which the quenching of $OH(A^2\Sigma^+)$ occurs to form $OH(X^2\Pi_i)$. For some partners, collisions with $OH(A^2\Sigma^+)$ can potentially lead to reactive channels (e.g., for N_2 the product channels $H + N_2O$ and $NH + NO$ are accessible) but these have not been identified in the ab initio calculations [19]. However, in order to test the accuracy of these potential surfaces, dynamical calculations are required under full collision conditions to predict the cross-sections for quenching, but these have not been performed. No ab initio potential surface has been calculated for OH–H_2O interactions.

There have been several conceptual models considered to describe collisional quenching [20]. The Parmenter–Seaver (PS) well-depth correlation has enjoyed only limited success [16,21]. Better agreement with both the magnitude and temperature dependence of quenching cross-sections was achieved using a collision complex model with the long-range part of the potential energy surface described by the sum of attractive multipole interactions (dipole–dipole, dipole–quadrupole, dipole-induced–dipole and dispersion) and a repulsive centrifugal barrier [16,22,23]. Such a model predicts an inverse power law for the temperature dependence, as observed experimentally at lower temperatures, but predicts an approximately gas-kinetic cross-section for all collision partners – even though many species do not appear to quench at all. The collision complex model only describes a small part of the approach of the collision partners, and does not contain any quenching mechanism. The 'harpooned' mechanism, developed by Paul [8], postulates that quenching occurs via an ion-pair intermediate:

$$OH(A^2\Sigma^+) + M \rightarrow OH^-(X^1\Sigma^+) + M^+ \rightarrow OH(X^2\Pi_i) + M, \quad (1)$$

involving crossings with a surface associated with OH^- and the positive ion of the collision partner. Once the pair is brought to a radius where transfer can occur, then transfer occurs irreversibly. This model predicts a relatively constant cross-section above 1000 K, as observed for many colliders, and predicts that many species are weak or non-quenchers of $OH(A^2\Sigma^+,\ v' = 0)$ [8]. A combination of the collision complex and harpooned model, with additional account taken of the rotational level dependence of the quenching cross-section using an exponential energy gap law [24], was able to predict the quenching behaviour for some colliders at low temperatures [25], but discrepancies were observed, and are likely due to a failing of the collision complex model at low temperatures. In this Letter the idea of a collision complex is abandoned completely, and an analytical expression is derived for the quenching cross-section in terms of the potential. The new approach appears to work well at low and high temperatures and, in this Letter, is compared to the quenching data for H_2O over a wide range of temperatures.

2. Experimental

The discharge-flow LIF system for the production and detection of OH was described previously [25] and only details pertinent to quenching measurements with water vapour are reproduced here. Briefly, OH was generated by the fast reaction between H atoms and NO_2 at a total pressure of 2 Torr in He buffer gas. Water vapour was introduced into the fluorescence cell as follows. A controlled flow of He was bubbled through distilled and de-ionised water (Whatman Stillplus, resistivity $> 14\ M\Omega\ cm^{-1}$) in a Drechsel bottle for at least 30 min to remove any dissolved O_2 and N_2, at a total pressure of ~ 600 Torr (MKS Baratron). The gas temperature and relative humidity were monitored by a humidity probe (Vaisala HMP 230 Series), and together with the measured pressure were used to calculate the vapour pressure of H_2O in the flow exiting the Drechsel bottle. Following passage through a calibrated mass flow controller (Tylan General FC280) the He/H_2O was introduced sufficiently upstream of the detection region to allow thorough mixing. The partial pressure over which H_2O could be varied during an experiment was limited by the saturated vapour pressure of H_2O, and the following pressure ranges were used to avoid condensation onto the cell walls: 0–58 mTorr (236–294 K), 0–20 mTorr (227–236 K), and

0–10 mTorr (211–227 K). OH was detected by LIF, using < 10 μJ pulse^{-1} in a 3-mm-diameter beam at 307.995 nm to excite OH to the $A^2\Sigma^+$ ($v' = 0$, $N' = 2$, $J' = 2.5$) state via excitation of the $Q_1(2)$ line. The resulting fluorescence decay was digitised at 10 ns resolution and averaged over 400–1000 laser shots. Gases used: He, BOC CP grade (99.999%), H_2, BOC CP grade (99.995%), NO_2 BDH (99.5%).

3. Results

The contribution to quenching of OH by the H_2 and NO_2 used to generate OH is negligible at the pressures used [11]. The fluorescence signals were fitted to a single exponential decay, from which the decay constant was obtained. By using 2 Torr of He buffer rotational relaxation of the excited OH($A^2\Sigma^+$, $v' = 0$) should be complete in ~ 200 ns and hence only that part of the decay for $t > 200$ ns was used in the analysis [25]. The decay constants were determined at a variety of concentrations of H_2O, from which the rate constant for quenching $k_Q(T)$ was determined using the expression:

$$\tau^{-1} = A_f + k_Q(T)\,[H_2O], \qquad (2)$$

where τ^{-1} is the decay constant and A_f is the Einstein coefficient for spontaneous emission. Fig. 1 shows the H_2O pressure dependence of the decay constants at 293, 263 and 243 K together with linear least-squares fits of Eq. (2) to the data. The intercept

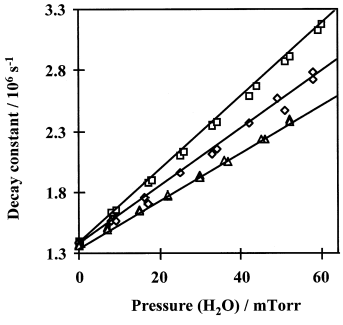

Fig. 1. Second-order plots illustrating the fluorescence decay constants as a function of added water vapor at $T = 243$ K (□), $T = 263$ K (◇) and $T = 293$ K (△). Although not shown in the figure for reasons of clarity, the errors in the decay constant and H_2O partial pressure are 3% and 6%, respectively.

Table 1
Rate constants and cross-sections for quenching of OH($A^2\Sigma^+$, $v' = 0$) by H_2O

Temperature[a] (K)	$k_Q(T)$ (10^{-10} cm^3 molecule^{-1} s^{-1})	$\sigma_Q(T)$[b] (Å^2)
294	6.91 ± 0.5[c]	81.9 ± 6[c]
283	6.79 ± 0.7	82.0 ± 8
273	6.74 ± 0.7	82.9 ± 8
263	6.94 ± 0.7	86.9 ± 9
253	7.38 ± 0.7	94.3 ± 9
245	7.44 ± 0.7	96.6 ± 10
236	7.77 ± 0.8	103 ± 10
227	7.85 ± 0.8	106 ± 11
219	8.09 ± 0.8	111 ± 11
211	8.49 ± 0.8	119 ± 12

[a] The error in the temperature is ± 1 K.
[b] $\sigma_Q(T) = k_Q(T)/\langle v \rangle$, where $\langle v \rangle$ is the average velocity, given by $\langle v \rangle = (8RT/\pi\mu)^{1/2}$, and μ is the reduced mass of the collision.
[c] An average of five values determined between 293 and 295 K.

is consistent with the OH($A^2\Sigma^+$, $v' = 0$) radiative lifetime [10]. Table 1 lists the measured rate constants, $k_Q(T)$, and the thermally averaged cross-sections, $\sigma_Q(T)$, for all temperatures studied, and Fig. 2 plots the values of $\sigma_Q(T)$. For each temperature 16 concentrations of H_2O were used to determine the quenching rate constant, and the quoted errors are dominated by the systematic error in calculating the concentration of H_2O.

4. Discussion and model calculations

Table 1 and Fig. 2 indicate that the quenching cross-sections are very large, being greater than the hard-sphere cross-section for collisions of OH and

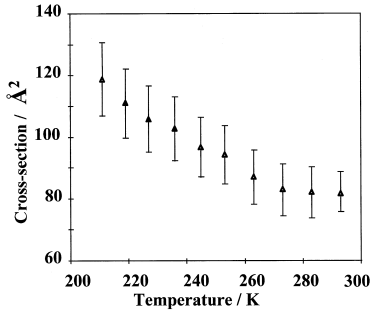

Fig. 2. Temperature dependence of the cross-section for quenching of OH ($A^2\Sigma^+$, $v' = 0$) by H_2O.

H_2O. Together with the observed negative dependence of $\sigma_Q(T)$ on temperature ($\sim 45\%$ increase between 294 and 211 K), this provides strong evidence that attractive forces control the quenching process at low temperatures. Although no data exist for comparison below room temperature, there have been a number of measurements performed in flames [15,17] and laser-heated cells [16], in which the quenching cross-section was found to be essentially independent of temperature between 1000 K (~ 30 Å^2) and 2300 K (~ 25 Å^2).

Although the 'harpooned' process provides a mechanism for understanding how quenching occurs, and is able to predict the relative efficiencies for various collision gases, it is calculated to have virtually no temperature dependence [8]. At low temperatures the coming together may dominate the temperature dependence of the quenching process and, in order to predict the observed temperature dependence, the model must incorporate a realistic potential energy surface which brings the partners together. The simple collision complex model poorly represents the temperature dependence at low temperatures [16,23], and in this section it is abandoned altogether in favour of a different approach.

For a point centers potential, the distance of closest approach, r_m, is found by solving [26]:

$$1 - \frac{2\varphi(r_m)}{M v^2} - \frac{b^2}{r_m^2} = 0, \tag{3}$$

for the largest root as a function of the impact parameter, b, and the relative velocity, v, where M is the reduced mass of the colliding pair and $\varphi(r_m)$ is the intermolecular potential at distance r_m. The largest impact parameter for which the distance of closest approach is the Harpoon(ed) radius, r_H, is then given by:

$$b_H^2 = r_H^2\left(1 - \frac{\varphi(r_H)}{\eta kT}\right), \tag{4}$$

where $\eta \equiv M v^2/2T$, and k is the Boltzmann constant. The thermally averaged quenching cross-section is given by:

$$\langle \sigma \rangle = \pi \int_0^\infty \eta \exp(-\eta) \int_0^\infty P(\eta, b)\, \mathrm{d}b^2\, \mathrm{d}\eta, \tag{5}$$

where P is the probability for quenching. Paul [8] suggested that when the harpooned process is strongly allowed, the quenching probability is a weak function of the initial conditions for the collision. Thus, to lowest order the harpooned quenching probability is taken as a constant, P_H, for all collisions reaching r_H or closer, and zero otherwise. Such an approach yields an analytical expression for $\langle \sigma \rangle$:

$$\langle \sigma \rangle = \pi r_H^2 P_H\left(1 - \varphi(r_H)/kT\right). \tag{6}$$

It should be noted that for a value of r_H located in the attractive portion of the potential, the potential is negative and thus the cross-section decreases with increasing temperature and becomes constant at high temperatures.

Both water and OH($A^2\Sigma^+$) display relatively large dipole moments (2.0 D for OH), and thus we consider a Lennard-Jones potential modified to include dipole moment effects [27]:

$$\varphi(r) = 4\varepsilon_{ij}\left[\left(\frac{\sigma}{r}\right)^{12} - \left(\frac{\sigma}{r}\right)^{6}\left(1 + \frac{\mu_i^2\alpha_j + \mu_j^2\alpha_i}{4\varepsilon_{ij}\sigma^6} + \frac{2\gamma}{3}\frac{\mu_j^2\mu_i^2}{4\varepsilon_{ij}\sigma^6 kT}\right)\right], \tag{7}$$

where μ and α are the molecular dipole moments and polarizabilities, respectively, of the colliding species i and j. Eq. (7) may be extended to include a dipole–quadrapole term which is proportional to $1/(r^8 kT)$. This term had little effect on the model predictions and was thus not included in the results presented here. It is common to take the value of $\gamma = 1$. However, as noted by Gray and Gubbins [28], Eq. (7) is in fact the result of truncating a series expansion and a value of $(1/4) < \gamma < (1/2)$ is required to match the lowest order terms of this series (i.e., Eq. (7)) to a series expansion for a fluid having a true effective central potential.

The harpooned radius was computed using molecular parameters for OH($A^2\Sigma^+$) and the procedure given by Paul [8]. The relationships for calculating the crossing radius [8] suggest an energetically ac-

cessible crossing from $OH(A^2\Sigma^+,\ v=0)+H_2O$ to $OH^-(X^1\Sigma^+,\ v=0)+H_2O^+$, although there are no ab initio or experimental studies to support the existence of such a crossing. For H_2O the dipole moment and polarizability were taken as 2.673 D and 1.847 Å^3, respectively. For H_2O the Lennard-Jones parameters were taken as $\varepsilon = 535.21$ K and $\sigma =$ 2.673 Å as obtained from fitting low-density viscosity data using a potential of the form of Eq. (7) [29]. For OH the Lennard-Jones parameters were set at the values estimated for $OH(X^2\Pi_i)$, $\varepsilon = 281.27$ K and $\sigma = 3.111$ Å [29]. The pair Lennard-Jones parameters were computed following the prescription of Bzowski et al. [30]. The value of $\gamma = 1/4$ was taken based on the observation by Paul [29] that this provides the best representation of pure species low-density viscosity data as tested for a wide range of polar compounds.

Fig. 3a shows the available experimental data for quenching of $OH(A^2\Sigma^+,\ v'=0)$ by water vapour in the range 200–2500 K, and Fig. 3b shows a subset of these data below 400 K. Also plotted in Fig. 3a,b are four different model predictions for the quenching cross-sections as given by: (i) Paul [8] which is based on a combined harpoon/collision complex model; (ii) Tamura et al. [15] which is an empirical fit to a PS model; (iii) Garland and Crosley [23] which is a pure collision complex model; and (iv) the model described in Eqs. (6) and (7) above with a value of $P_H = 0.67$ set by matching the 300 K data point of Wysong et al. [11].

As noted by Paul [8] the pure collision complex model does not capture the relative temperature independence found at higher temperatures, whereas this behavior is captured by both the harpoon- and PS-based models. The well depth parameter, (ε/k) obtained by Tamura et al. [15] in fitting to a PS model, is 434 K, as compared to the effective well depth of 382 K used in the model potential described above. At lower temperature the collision complex-based models [23] display a power law character of the form $T^{-2/3}$ and the PS model has a strong exponential character (i.e., $\exp(\varepsilon/kT)$) in temperature. These do not appear to capture the observed low temperature dependence in the cross-section. In contrast, the simple model described above works well; however, this agreement is lost in setting the contribution of the dipole–dipole term to zero.

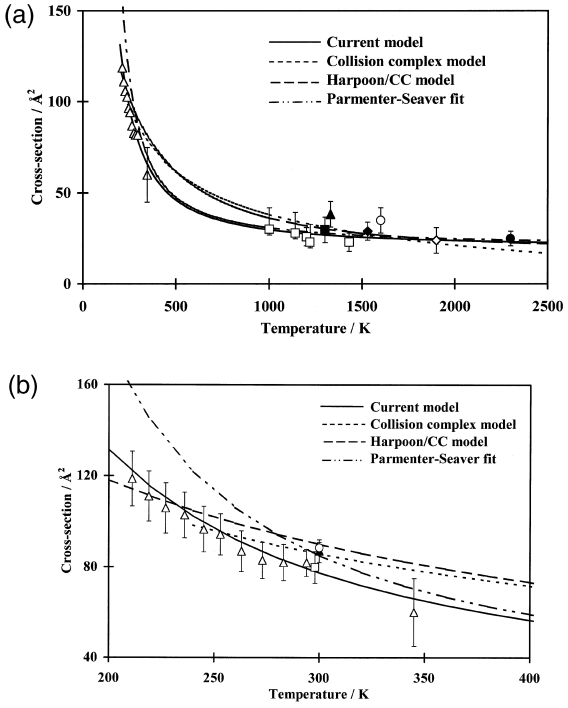

Fig. 3. (a) Comparison of the measured and modelled cross-sections for quenching of $OH(A^2\Sigma^+,\ v'=0)$ by H_2O in the range 200–2500 K. △, This work (error bars omitted for clarity except for the data point at 345 K, which was obtained in this laboratory from an intercept during an experiment which employed H_2O as a source as OH); □, Fairchild et al. [16]; ■, Carrington [31]; ◇, Stepowski and Cottereau [32] (extracted from flame data using high-temperature O_2 and CO_2 cross-sections measured by Paul et al. [33]); ●, Jeffries et al. [17]; ◆, Kienle et al. [34]; ○, Harleid et al. [35]; ▲, Lee et al. [36] (extracted from flame data). (b) Comparison of the measured and modelled cross-sections for quenching of $OH(A^2\Sigma^+,\ v'=0)$ by H_2O below 400 K. △, This work; □, Wysong et al. [11]; ▲, Cleveland and Wiesenfeld [12]; ○, Copeland and Crosley [13] (extracted from N-dependent data).

The model developed here can be written in the general form:

$$\langle \sigma \rangle = \sigma_\infty \left(1 + \frac{A}{kT}\left(1 + \frac{B}{kT}\right)\right), \qquad (8)$$

where $\sigma_\infty = \pi r_H^2 P_H$ is the high-temperature limiting cross-section and the constants A and B can be expressed in terms of the potential parameters (the later being non-negligible for polar–polar collision partners). This form has a significantly different temperature dependence than that obtained form either the collision complex or PS models. By con-

straining the parameters to physically meaningful quantities this simple functional form provides a physically based means to fit experimental data over a wide range of temperatures. The parameters obtained by fitting Eq. (8) to the results of the calculation using Eqs. (6) and (7) gives: $\sigma_\infty = 20.847$ Å^2, $A/k = 440.82$ K, and $B/k = 271.77$ K.

Several features of these models become evident upon comparison with experimental data. The collision complex model predicts a temperature dependence that is too weak below 1000 K, and a continued decrease in cross-section at very high temperatures. The addition of the harpooned process to this model corrects this discrepancy above 1500 K. The PS model, with parameters chosen to match the relative temperature independence above 1000 K, provides too strong a temperature dependence below 300 K. The model presented here appears to successfully capture both the low- and high-temperature behavior measured for quenching of OH by water vapour.

5. Conclusions

Cross-section measurements have been made below room temperature for electronic quenching of $OH(A^2\Sigma^+,\ v' = 0)$ by H_2O. The cross-section increases by $\sim 45\%$ upon decreasing the temperature from 292 to 211 K, consistent with attractive forces dominating the collision process. Together with cross-sections obtained at higher temperatures, the low-temperature data have been compared with the predictions of a number of models which describe the quenching process. At high temperatures (> 1000 K), the observed cross-sections are relatively invariant with temperature, in contrast to the collision complex model, but it is difficult to distinguish between the accuracy of the other models. However, the predictions of the models deviate significantly from each other at the low temperatures of this study, and poor agreement was found between the experimental temperature dependence and the predictions of a simple collision-complex model, a model based on PS correlations, and a harpooned process coupled with the formation of a collision complex. Much better agreement over the entire temperature range was achieved with a new model that is described in this Letter. The model is based on the harpooned process but abandons the concept of a collision complex in favor of a simple description of the collision, where approach occurs upon a Lennard-Jones intermolecular potential modified to include dipole moment effects. In combustion and atmospheric media water vapour is often the dominant quenching species, and parameterization of the model expression enables the cross-section to be calculated at any temperature of interest, allowing the effects of quenching to be corrected with a high degree of confidence.

Acknowledgements

DEH is grateful to the Royal Society for the award of a University Research Fellowship and for some equipment funding. AEB and DAH are grateful to the NERC and EPSRC, respectively, for the award of Research Studentships. PHP acknowledges the support of the US Department of Energy, Office of Basic Energy Sciences, Chemical Sciences Division.

References

[1] K. Kohse-Hoinghaus, J.B. Jeffries, R.A. Copeland, G.P. Smith, D.R. Crosley, 22nd Symposium (International) on Combustion, The Combustion Institute, Pittsburgh, PA, 1988, p. 1857.
[2] D.R. Crosley, J. Atmos. Sci. 52 (1995) 3299.
[3] D.R. Crosley, J. Atmos. Sci. 52 (1995); entire issue devoted to NO_x measurements, in particular pp. 3238, 3393, 3413, 3428.
[4] D.E. Heard, J.B. Jeffries, G.P. Smith, D.R. Crosley, Combustion Flame 88 (1992) 137.
[5] S.A. McKeen, G. Mount, F. Eisele, E. Williams, J. Harder, P. Goldan, W. Kuster, S.C. Lui, K. Baumann, D. Tanner, A. Fried, S. Sewell, C. Cantrell, R. Shetter, J. Geophys. Res. 102 (1997) 6467.
[6] P.O. Wennberg, T.F. Hanisco, R.C. Cohen, R.M. Stimpfle, L.B. Lapson, J.G. Anderson, J. Atmos. Sci. 52 (1995) 3413.
[7] D.J. Creasey, P.A. Halford-Maw, D.E. Heard, M.J. Pilling, B.J. Whitaker, J. Chem. Soc. Faraday. Trans. 93 (1997) 2907.
[8] P.H. Paul, J. Quant. Spectrosc. Radiat. Transfer 51 (1994) 511.
[9] P.H. Paul, C.D. Carter, J.A. Gray, Sandia National Laboratories, Report No. SAND 94-8244, 1994.
[10] K. Schofield, J. Phys. Chem. Ref. Data 8 (1979) 723.

[11] I.J. Wysong, J.B. Jeffries, D.R. Crosley, J. Chem. Phys. 92 (1990) 5218.
[12] C.B. Cleveland, J.R. Wiesenfeld, Chem. Phys. Lett. 144 (1988) 479.
[13] R.A. Copeland, D.R. Crosley, Chem. Phys. Lett. 107 (1984) 295.
[14] I.S. McDermid, J.B. Laudenslager, J. Chem. Phys. 76 (1982) 1824.
[15] M. Tamura, P.A. Berg, J.E. Harrington, J. Luque, J.B. Jeffries, G.P. Smith, D.R. Crosley, Combustion Flame, 1998, in press.
[16] P.W. Fairchild, G.P. Smith, D.R. Crosley, J. Chem. Phys. 79 (1983) 1795.
[17] J.B. Jeffries, K. Kohse-Hoinghaus, G.P. Smith, R.A. Copeland, D.R. Crosley, Chem. Phys. Lett. 152 (1988) 160.
[18] S.M. Miller, D.C. Clary, A. Kliesch, H.J. Werner, Mol. Phys. 83 (1994) 405.
[19] M.I. Lester, R.A. Loomis, B.L. Schwartz, S.P. Walch, J. Phys. Chem. A 101 (1997) 9195.
[20] D.R. Crosley, J. Phys. Chem. 93 (1989) 6279.
[21] H.-M. Lin, M. Seaver, K.Y. Tang, A.E.W. Knight, C.S. Parmenter, J. Chem. Phys. 70 (1979) 5442.
[22] D.L. Holtermann, E.K.C. Lee, R. Nanes, J. Chem. Phys. 77 (1982) 5327.
[23] N.L. Garland, D.R. Crosley, 21st Symposium (International) on Combustion, The Combustion Institute, Pittsburgh, PA, 1986, p. 1693.
[24] R.A. Copeland, M.J. Dyer, D.R. Crosley, J. Chem. Phys. 82 (1985) 4022.
[25] A.E. Bailey, D.E. Heard, P.H. Paul, M.J. Pilling, J. Chem. Soc. Faraday Trans. 92 (1997) 2915.
[26] S. Chapman, T.G. Cowling, The Mathematical Theory of Non-Uniform Gases, Cambridge University Press, 1979.
[27] J.O. Hirschfelder, C.F. Curtiss, R.B. Bird, Molecular Theory of Gases and Liquids, Wiley, New York, 1954.
[28] C.G. Gray, K.E. Gubbins, Theory of Molecular Fluids; Fundamentals, Vol. 1, Oxford, Clarendon, 1984.
[29] P.H. Paul, DRFM: a New Package for the Evaluation of Gas-Phase-Transport Properties, Sandia National Laboratories Report SAND98-8203, 1997.
[30] J. Bzowski, J. Kestin, E.A. Mason, F.J. Uribe, J. Phys. Chem. Ref. Data 19 (1990) 1179.
[31] T. Carrington, J. Chem. Phys. 30 (1959) 1087.
[32] D. Stepowski, M. Cottereau, Combustion Flame 40 (1981) 65.
[33] P.H. Paul, J.L. Durant Jr., J.A. Gray, M.R. Furlanetto, J. Chem. Phys. 102 (1995) 8378.
[34] R. Kienle, M.P. Lee, K. Kohse-Hoinghaus, Appl. Phys. B 62 (1989) 583.
[35] A.T. Harleid, D. Markus, W. Kreutner, K. Kohse-Hoinghaus, Appl. Phys. B 65 (1997) 81.
[36] M.P. Lee, R. Kienle, K. Kohse-Hoinghaus, Appl. Phys. B 58 (1994) 447.